

# Femtoscopy analysis of d-Au interactions at $\sqrt{s} = 200\text{GeV}$

Piotr Bożek<sup>1,2,\*</sup>

<sup>1</sup>*AGH University of Science and Technology, Faculty of Physics and Applied Computer Science, al. Mickiewicza 30, PL-30059 Krakow, Poland*

<sup>2</sup>*The H. Niewodniczański Institute of Nuclear Physics, Polish Academy of Sciences, PL-31342 Kraków, Poland*

(Dated: August 7, 2014)

The femtoscopy correlation radii for d-Au collisions at 200GeV are calculated in the hydrodynamic model and compared to PHENIX collaboration data. For asymmetric systems, such as d-Au or p-Pb collisions, the correlation radius  $R_{out-long}$  is estimated and predicted to be non-zero. It appears due to different lifetimes of the parts of the fireball at positive and negative rapidities. Azimuthally sensitive Hanbury Brown-Twiss analysis with respect to the second order event plane shows a significant angular dependence of the radii. It reflects the strong azimuthal asymmetry of the d-Au source geometry and flow for central interactions.

PACS numbers: 25.75.-q, 25.75.Gz, 25.75.Ld

## I. INTRODUCTION

The dynamics of ultrarelativistic collisions between a large nucleus and a smaller projectile is the subject of intensive experimental and theoretical studies [1]. One of the key characteristic of the system is the size of the interaction region [2–4]. The PHENIX collaboration published results on the Hanbury Brown-Twiss (HBT) correlations for d-Au collisions at 200GeV [5]. The results are for three HBT radii side  $R_{side}$ , out  $R_{out}$ , and long  $R_{long}$  ( $R_{s,o,l}$ ) as function of the pion pair momentum and for different collision centralities. Previously the PHENIX experiment presented results indicating collective flow effects in the dynamics of d-Au collisions [6]. The density of matter created in central d-Au interactions is similar as in Au-Au collisions, which implies a collective expansion stage. Combined with the large eccentricity of the fireball in d-Au collisions it leads to a significant elliptic flow of emitted particles [7]. In the hydrodynamic model hadrons are emitted from the freeze-out hypersurface and the femtoscopy radii measure the size of the effective emission region (the homogeneity region). The collective expansion of matter leads to strong space-momentum correlations for the emitted particles. The size of the homogeneity region measured with pion interferometry diminishes with increasing average pion pair momentum [8].

In central collisions of asymmetric systems, such as d-Au and p-Pb collisions, the charged particle density in rapidity is far from boost invariance and is not symmetric in the central rapidity region [9, 10]. The fireball formed in the collision is asymmetric in space-time rapidity, on the side of the larger nucleus it lives longer. In the following, it is shown that an additional radius parameter appears in the Gaussian form of the interferometry correlations function, representing a mixed out-long correla-

tions term. The value of the  $R_{out-long}^2$  ( $R_{ol}^2$ ) parameter is predicted for d-Au and p-Pb collisions.

The azimuthal asymmetry of the emitting source can be observed using the method of azimuthally sensitive HBT correlations [11, 12]. In particular, the spatial eccentricity should be visible as an increase of the side radius extracted for pion pairs emitted in plane. The azimuthal dependence of the interferometry radii with respect to the second order event plane involves even harmonics in its Fourier decomposition. In Sect. V, it is shown that for a system with strong quadrupole deformation, as in d-Au collisions, the second harmonic component can be identified for all the three HBT radii.

## II. HBT RADII

The dynamics of d-Au and Au-Au collisions is described using the event-by-event 3 + 1-dimensional viscous hydrodynamic model [13]. The initial density of the fireball formed in the collision is modeled using the Glauber Monte Carlo model [14]. For each initial density profile, the expansion is followed using viscous hydrodynamics with shear and bulk viscosity. The viscosity to entropy ratio is fixed at 0.08 for the shear and 0.04 for bulk viscosity [15]. At the freeze-out temperature of 150MeV the collective expansion stops and particles are emitted, with subsequent resonance decays [14]. Due to limited statistics that can be obtained in the simulations, for each hydrodynamic freeze-out hypersurface 5000 real events are generated and combined together to increase statistics. It means that the number of pion pairs per event is effectively increased 5000 times.

The correlation function  $C(q, k)$  for a pion pair of average momentum  $k$  and relative momentum  $q$  is approx-

---

\* Piotr.Bozek@ifj.edu.pl

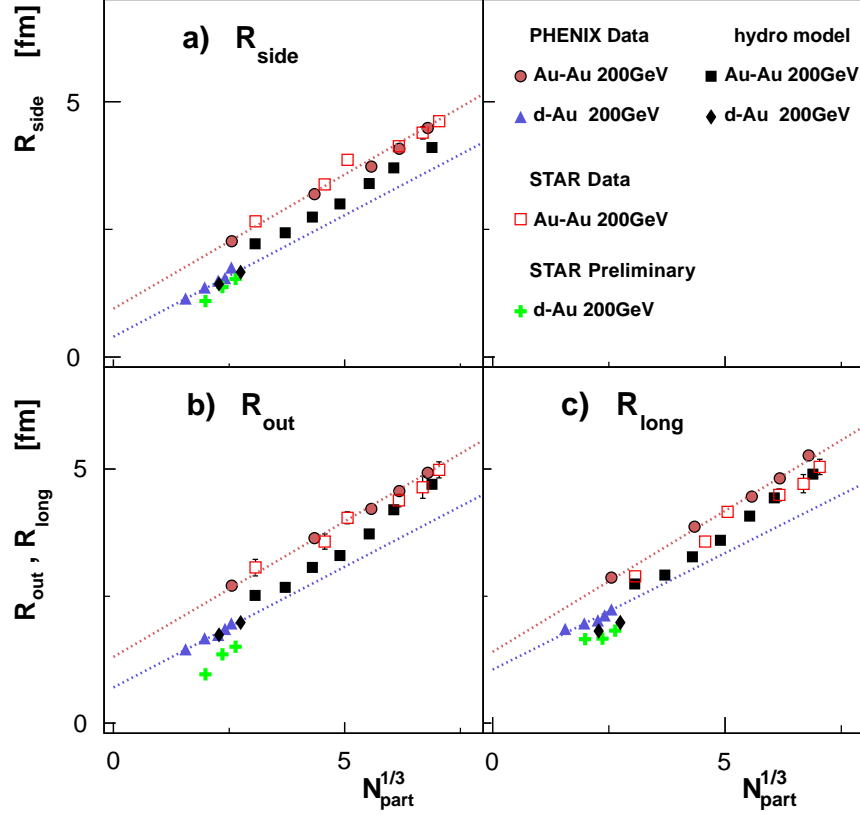


FIG. 1. The HBT radii  $R_{side}$  (panel a)),  $R_{out}$  (panel b)), and  $R_{long}$  (panel c)) for d-Au and Au-Au collisions at 200GeV for different centralities (plotted as function of  $N_{part}^{1/3}$ ). The experimental data of the PHENIX collaboration are represented using circles (Au-Au) [16] and up-triangles (d-Au) [5], the Au-Au data of the STAR collaboration using open squares [17], and the preliminary d-Au data of the STAR collaboration using crosses [18]. The results of the hydrodynamic model are shown using diamonds (d-Au) and solid squares (Au-Au) [19]).

imated by a histogram  $C(q, k)$  in a bin  $q_a, k_b$  [19]

$$C(q_a, k_b) = \frac{\frac{1}{N_{pairs,num}} \sum_{j=1}^{N_h} \sum_{m,l=1}^{N_e} \sum_{s=1}^{M_l} \sum_{f=1}^{M_m} \delta_{q_a} \delta_{k_b} \Psi(q, x_1 - x_2)}{\frac{1}{N_{pairs,den}} \sum_{i \neq j=1}^{N_h} \sum_{l,m=1}^{N_e} \sum_{s=1}^{M_l} \sum_{f=1}^{M_m} \delta_{q_a} \delta_{k_b}} \quad (2.1)$$

The numerator is constructed summing over events  $l$  and  $m$  generated from the same freeze-out hypersurface  $j$  ( $M_l$  and  $M_m$  are the multiplicities of the respective events), in the denominator the two events are generated from two different hydrodynamic events  $i$  and  $j$ . If the relative momentum  $q = p_s - p_f$  and the average pair momentum  $k = (p_s + p_f)/2$  fall into the respective bins,  $\delta_{q_a}$  and  $\delta_{k_b}$  are 1 and 0 otherwise.  $\Psi(q, x_1 - x_2) = (e^{iq(x_1 - x_2)} + e^{-iq(x_1 - x_2)})/\sqrt{2}$  is the symmetrized wavefunction of the pion pair. Final state interactions between pions, are not taken into account in the above formula and no corrections for such interactions are performed when fitting the Gaussian formula to the correlation function. The correlation function is constructed in the longitudinal comoving system for pion pairs with

rapidity  $|y| < 1$ . The details of the procedure for the hydrodynamic evolution and for the construction of the HBT correlation function in the event-by-event hydrodynamic model can be found in [2, 19].

In a given average transverse pair momentum  $k_\perp$  bin, the dependence of the correlation function  $C(q, k_\perp)$  on the relative momentum  $q$  is decomposed into three components,  $q_l$  along the beam axis,  $q_o$  along the pair transverse momentum  $k_\perp$  in the local comoving system, and  $q_s$  orthogonal to the first two directions. The Bertsch-Pratt formula is fitted in 3-dimensions

$$C(q, k_\perp) = 1 + \lambda e^{-R_o^2 q_o^2 - R_s^2 q_s^2 - R_l^2 q_l^2}, \quad (2.2)$$

where the extracted parameters  $R_{o,s,l}$  are the three HBT radii [20].

In Fig. 1 is shown the dependence of the HBT radii on the average number of participant nucleons for the given centrality class, for  $350 \text{ MeV} < k_\perp < 450 \text{ MeV}$ . The calculation reproduces rather well the experimental data of the PHENIX collaboration for d-Au collisions. The preliminary STAR collaboration results for  $R_o$  in d-Au are below the PHENIX results. The systematic uncertainty of the fitted results for the hydrodynamic calcu-

lation is estimated by varying the range of the fit from  $|q| < 0.1\text{GeV}$  to  $0.2\text{GeV}$ , the variation of the extracted radii is smaller than 10%.

The calculated radii for Au-Au collisions are systematically below the experimental values. The deviation is not reduced by lowering the freeze-out temperature to  $140\text{MeV}$ . The result shows that the hydrodynamic model can describe only partly the dependence of the HBT radii on the system size and the centrality of the collisions. It may indicate that the flow profile generated in the hydrodynamic simulation with Glauber model initial conditions is only approximate or that contributions of the pre-equilibrium flow or rescattering stage are noticeable [21]. Other effects could be also be important for the interferometry in small systems [22].

### III. AZIMUTHALLY SENSITIVE HBT CORRELATION FUNCTION IN ASYMMETRIC COLLISIONS

In this section I recall the basic formulae of the azimuthally sensitive HBT analysis [11] and apply them to the correlation function with respect to the second order event-plane, for a system without forward-backward symmetry in rapidity. The azimuthal dependence of the HBT correlation function comes from the explicit dependence on the angle  $\Phi$  between the emitted pion pair with respect to the event-plane and from the implicit dependence of the emission function  $S(x, k)$  on the angle [11, 12]. For a general Gaussian parametrization of the correlation function

$$C(q, k) = 1 + \lambda e^{-\sum_{i,j} R_{i,j}^2 q_i q_j} \quad , \quad i = o, s, l \quad , \quad (3.1)$$

the radii parameters  $R_{i,j}^2$  are related to moments of the emission function  $S(x, k)$ ,  $S_{\mu\nu} = \langle x_\mu x_\nu \rangle - \langle x_\mu \rangle \langle x_\nu \rangle$ ,  $z$  is along the beam direction,  $(x, y)$  is the transverse plane, the second order flow direction is  $x$ . The symmetries of the emission function  $S(x, k)$  can be used to infer the form the azimuthal dependence of the HBT radii [12]. In central p-Pb and d-Au collisions the fireball exhibits elliptic and triangular deformation. For p-Pb collisions it occurs solely due to fluctuations, while for d-Au collisions, even a zero impact parameter, the intrinsic deformation of the deuteron dominates the fireball eccentricity. In any case, the azimuthal angle is defined with respect to second order event plane in each event. In the average over many events, while keeping always the orientation with respect to the second order plane, one is left with two symmetries of the emission source

$$\begin{aligned} S(x, y, z, k_\perp, \Phi) &= S(x, -y, z, k_\perp, -\Phi) \\ S(x, y, z, k_\perp, \Phi) &= S(-x, y, z, k_\perp, \pi - \Phi) \quad . \end{aligned} \quad (3.2)$$

The Fourier expansion of the emission source moments respecting the symmetry is

$$\begin{aligned} \frac{1}{2} ((\langle x^2 \rangle - \langle x \rangle^2) + (\langle y^2 \rangle - \langle y \rangle^2)) &= A_0 + 2 \sum_{n=2,4,\dots} A_n \cos(n\Phi) \\ \frac{1}{2} ((\langle x^2 \rangle - \langle x \rangle^2) - (\langle y^2 \rangle - \langle y \rangle^2)) &= B_0 + 2 \sum_{n=2,4,\dots} B_n \cos(n\Phi) \\ \langle xy \rangle - \langle x \rangle \langle y \rangle &= 2 \sum_{n=2,4,\dots} C_n \sin(n\Phi) \\ \langle t^2 \rangle - \langle t \rangle^2 &= D_0 + 2 \sum_{n=2,4,\dots} D_n \cos(n\Phi) \\ \langle tx \rangle - \langle t \rangle \langle x \rangle &= 2 \sum_{n=1,3,\dots} E_n \cos(n\Phi) \\ \langle ty \rangle - \langle t \rangle \langle y \rangle &= 2 \sum_{n=1,3,\dots} F_n \sin(n\Phi) \\ \langle tz \rangle - \langle t \rangle \langle z \rangle &= G_0 + 2 \sum_{n=2,4,\dots} G_n \cos(n\Phi) \\ \langle xz \rangle - \langle x \rangle \langle z \rangle &= 2 \sum_{n=1,3,\dots} H_n \cos(n\Phi) \\ \langle yz \rangle - \langle y \rangle \langle z \rangle &= 2 \sum_{n=1,3,\dots} I_n \sin(n\Phi) \\ \langle z^2 \rangle - \langle z \rangle^2 &= J_0 + 2 \sum_{n=2,4,\dots} J_n \cos(n\Phi) \quad (3.3) \end{aligned}$$

The HBT parameters  $R_{i,j}^2(\Phi)$  of the Gaussian correlation function are obtained after rotation to the direction of the pair [8, 12]. The first terms of the Fourier expansion of the azimuthal dependence of the HBT radii are

$$\begin{aligned} R_s^2 &= A_0 - B_2 - C_2 + (2A_2 - B_0 - B_4 - C_4) \cos(2\Phi) \\ R_o^2 &= A_0 + B_2 + C_2 - 2E_1\beta_\perp - 2F_1\beta_\perp + D_0\beta_\perp^2 \\ &\quad + (2A_2 + B_0 + B_4 + C_4 - 2\beta_\perp(E_1 + E_3 - F_1 + F_3) \\ &\quad + 2D_2\beta_\perp^2) \cos(2\Phi) \\ R_{os}^2 &= (-B_0 + B_4 + C_4 + \beta_\perp(E_1 - E_3 - F_1 - F_3)) \\ &\quad \sin(2\Phi) \\ R_l^2 &= J_0 + 2J_2 \cos(2\Phi) \\ R_{ol}^2 &= H_1 + I_1 - G_0\beta_\perp + (I_1 + I_3 - H_1 + H_3) \cos(2\Phi) \\ R_{sl}^2 &= (I_1 + I_3 - H_1 + H_3) \sin(2\Phi) \quad , \end{aligned} \quad (3.4)$$

where  $\beta_\perp = k_\perp/k_0$ . The symmetry does not constraint the angle independent term of  $R_{ol}^2$  to vanish.

### IV. $R_{out-long}$ IN ASYMMETRIC COLLISIONS

In asymmetric collision one finds four angle independent radii parameters (Eq. 3.4) and the HBT correlation function has the form

$$C(q, k_\perp) = 1 + \lambda e^{-R_o^2 q_o^2 - R_s^2 q_s^2 - R_l^2 q_l^2 - 2R_{ol}^2 q_o q_l} \quad . \quad (4.1)$$

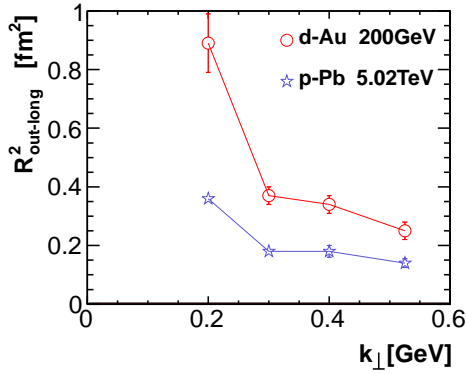


FIG. 2. The HBT radius  $R_{ol}^2$  for d-Au collisions at 200GeV (circles) and for p-Pb collisions at 5.02TeV (stars) as function of the pion pair momentum.

The radii are fitted to the angle averaged correlation function  $C(q, k_\perp)$  obtained from the hydrodynamic simulations, the same as used in the standard HBT analysis in Sect. II. The three radii  $R_o$ ,  $R_s$ , and  $R_l$  are the same as obtained with the simpler formula (2.2). However, one finds an asymmetry of the correlation function in the out-long direction, both in d-Au collisions at RHIC and p-Pb collisions at the LHC, which results in a nonzero value of  $R_{ol}^2$  (Fig. 2).

The nonzero value of  $R_{ol}^2$  for the correlation function in a symmetric window around midrapidity indicates that the fireball freezes out asymmetrically at positive and negative rapidities. On the side where the larger projectile goes, the fireball lives longer (we use the convention that the larger projectile moves with negative rapidity, which implies a positive value for the parameter  $R_{ol}^2$ ). In Fig. 3 is shown the density of the emission points for charged pions in d-Au collisions of centrality 0-5%. For this centrality the number of participant nucleons from the Au nucleus is much larger than the two participants from the deuteron [23]. The pion rapidity distribution is far from boost invariance and is strongly asymmetric in the forward-backward direction (Fig. 4). On the large nucleus going side (negative rapidity), the fireball is larger and lives longer. The emission time for pions with coordinates in the direction of the larger nucleus ( $z < 0$ ) is larger. As a consequence the moment  $G_0 = \langle zt \rangle - \langle z \rangle \langle t \rangle$  is negative, which leads to a nonzero contribution to the  $R_{ol}^2$  HBT radius.

The asymmetric radius  $R_{ol}^2$  is larger for collisions at lower energies. It is due to the fact that for central d-Au collisions at 200GeV the slope of the pion distribution in rapidity  $dN/dy$  at  $y = 0$  is larger than for p-Pb collisions at the LHC (Fig. 4). The time delay between pions emitted at negative and positive rapidities is larger for d-Au than for p-Pb collisions (Fig. 3). The distribution of emission points becomes more symmetric for pions with larger transverse momentum and the value of

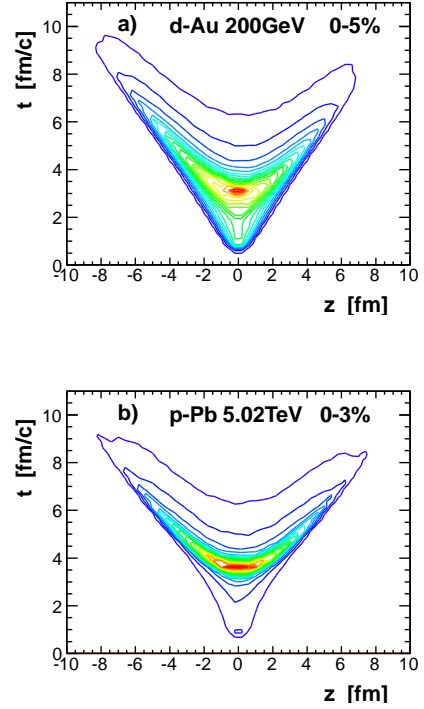


FIG. 3. The  $(z, t)$  emission point density of charged pions emitted in d-Au collisions at 200GeV (panel a) and p-Pb collisions at 5.02TeV (panel b), in the longitudinal comoving frame of the pion.

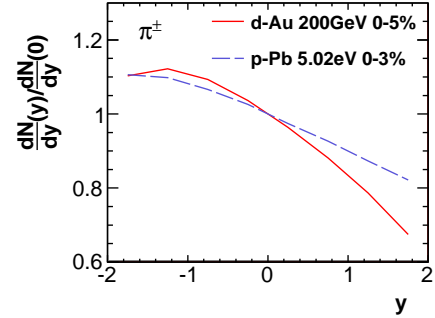


FIG. 4. The scaled rapidity distribution for charged pions in d-Au collisions at 200GeV (solid line) and p-Pb collisions at 5.02TeV (dashed line).

the forward-backward asymmetry in the emission time decreases.

## V. AZIMUTHALLY SENSITIVE HBT ANALYSIS

In the azimuthally sensitive HBT analysis with respect to the second order event plane, the correlation function

is calculated for pion pairs restricted to bins in the azimuthal angle. The azimuthal angle  $\Phi$  in the range  $[0, \pi]$  is subdivided into 6 bins. For each freeze-out hypersurface, the second order event plane angle  $\Psi_2$  is extracted from  $N_e = 5000$  combined events (each with multiplicity  $M_j$ )

$$v_2 e^{i2\Psi_2} = \frac{\sum_{j=1}^{N_e} \sum_{l=1}^{M_j} e^{i2\phi_l}}{\sum_{j=1}^{N_e} M_j}, \quad (5.1)$$

$\phi_l$  are the azimuthal angles of charged particles with  $|\eta| < 2$ . There is no correction for the event-plane resolution. On the other hand, the event-plane resolution may constitute a severe issue for the actual experimental analysis of the azimuthally sensitive HBT for d-Au collisions, where the multiplicity is relatively small.

The Gaussian fit functions for the each azimuthal angle and pair transverse momentum bin involves 5 radii parameters

$$C(q, k_\perp, \Phi) = 1 + \lambda e^{-R_o^2 q_o^2 - R_s^2 q_s^2 - R_l^2 q_l^2 - 2R_{ol}^2 q_o q_l - 2R_{os}^2 q_o q_s}. \quad (5.2)$$

The parameter  $R_{sl}^2$  is consistent with zero within the accuracy of the fit and is not considered in the analysis. The azimuthal dependence of the radii is described up to the second harmonic

$$\begin{aligned} R_o^2(\Phi) &= R_{o,0}^2 + 2R_{o,2}^2 \cos(2\Phi) \\ R_s^2(\Phi) &= R_{s,0}^2 + 2R_{s,2}^2 \cos(2\Phi) \\ R_l^2(\Phi) &= R_{l,0}^2 + 2R_{l,2}^2 \cos(2\Phi) \\ R_{os}^2(\Phi) &= 2R_{os,2}^2 \sin(2\Phi). \end{aligned} \quad (5.3)$$

For the out-long radius

$$R_{ol}^2(\Phi) = R_{ol,0}^2 + 2R_{ol,2}^2 \cos(2\Phi) \quad (5.4)$$

the second harmonic term  $R_{ol,2}^2$  could not be identified from the fit and in the following the azimuthal dependence of  $R_{ol}^2$  is not considered. The angle independent out-long parameter  $R_{ol,0}^2$ , due to forward-backward asymmetry, is discussed in Sect. IV.

The azimuthal angle dependence of the HBT radii for two transverse momentum bins is shown in Fig. 5. The dependence can be described using the zeroth and second harmonic as given by Eq. (5.3). The side radius is larger for the in plane direction, for pion pairs emitted in that direction the source size is dominated by the separation in the transverse plane between the proton and the neutron of the incoming deuteron. The fireball is wider when observed in plane, as the deuteron is preferably oriented out of plane. The out radius show the reverse behavior, it is smaller when viewed from the direction with the larger transverse flow.

The second order Fourier coefficients of the HBT radii with respect to the second order event plane are shown in Fig. 6. The second harmonic coefficients are fitted from the relation (5.3), correcting for finite bin width. The coefficient  $R_{o,2}^2$  is negative, while  $R_{s,2}^2$  is positive. The

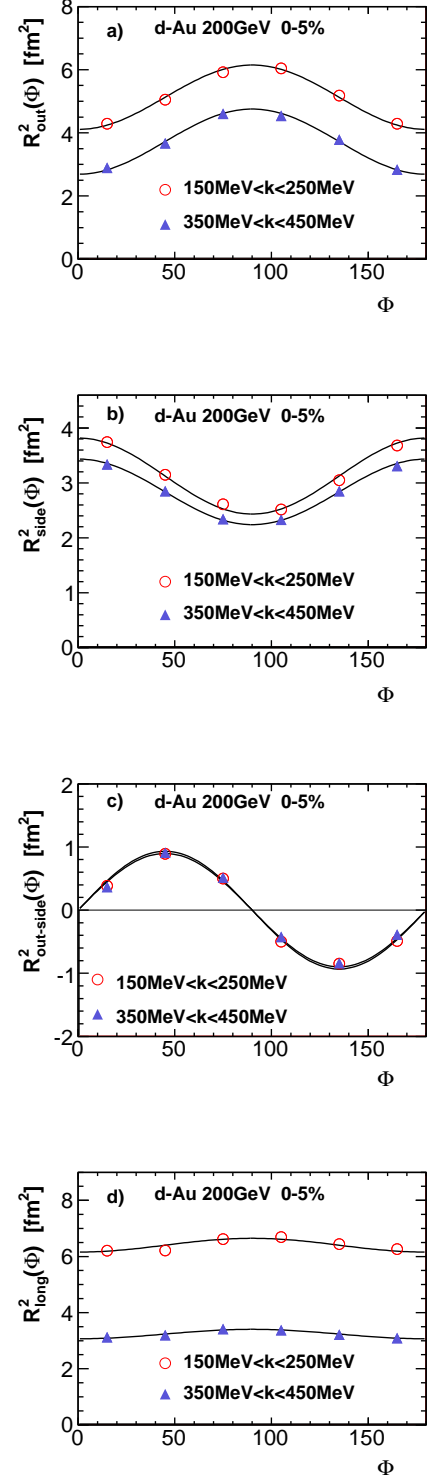


FIG. 5. (color online) The azimuthal angle dependence of the HBT radii  $R_o$  (panel a),  $R_s$  (panel b),  $R_{os}$  (panel c) and  $R_l$  (panel d) for  $150 \text{ MeV} < k_\perp < 250 \text{ MeV}$  (circles) and  $350 \text{ MeV} < k_\perp < 450 \text{ MeV}$  (triangles), the solid lines represent the second harmonic fit of the angular dependence of the radii (Eq. 5.3).



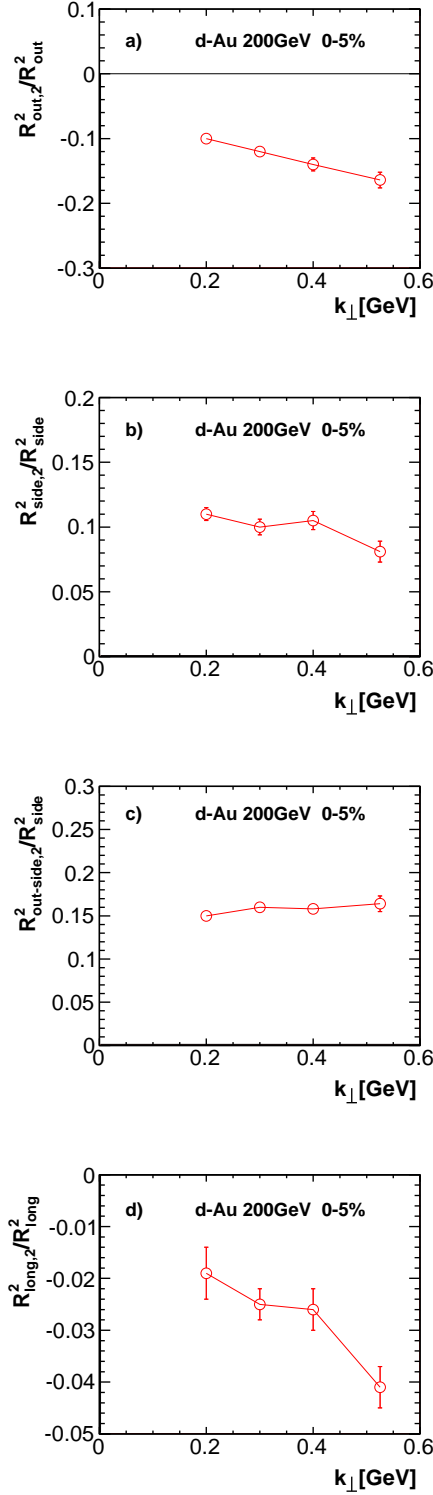


FIG. 6. Second order Fourier coefficients of the oscillations of the HBT radii with respect to the second order event plane for d-Au collisions at 200 GeV,  $R_{o,2}^2/R_{o,0}^2$  (panel a),  $R_{s,2}^2/R_{s,0}^2$  (panel b),  $R_{os,2}^2/R_{s,0}^2$  (panel c),  $R_{l,2}^2/R_{l,0}^2$  (panel d).

dependence on the pair momentum is weak. The large value of  $R_{s,2}^2$  reflects the dependence of the geometrical size of the emission source on the angle, in a very similar way as for nucleus-nucleus collisions at finite impact parameter [24].

For d-Au collisions at 0-5% centrality the second order harmonic in the azimuthal dependence of the HBT radii is very pronounced. For the strongly deformed fireball in d-Au collisions, both the shape and the flow at freeze-out have a large quadrupole anisotropy. The second order harmonic in the  $R_l$  radius, while it is smaller than for  $R_o$  and  $R_s$ , can be extracted from the identical pion correlation function. The asymmetry of the flow generates a contribution proportional to  $J_2$  in Eq. (3.4), that can be measured. If a similar sign and magnitude of  $R_{l,2}^2$  is observed in experiment, it would indicate that the viscous hydrodynamic model describes well the local flow and the pressure anisotropy at freeze-out.

## VI. SUMMARY

We present a study of HBT correlations for d-Au collisions at 200 GeV. The experimental analysis of the azimuthal correlations indicates that collective flow appears in such collisions. The interferometry analysis is performed on events generated in the viscous hydrodynamic model that describes the observed flow asymmetry [6]. The identical pion correlation function is constructed in bins of average transverse momentum of the pion pair. From a Gaussian fit to the correlation function, the HBT radii  $R_s$ ,  $R_o$ , and  $R_l$  are extracted. The values of the HBT radii are consistent with the experimental measurements [5]. The model underestimates the HBT radii for peripheral Au-Au collisions at the same energy. It may indicate that some details of the energy deposition in the fireball and of the flow profile are incorrect for the chosen Glauber model initial conditions, further effects may be due to pre-equilibrium flow or non-femtoscopic correlations that are unaccounted for in the model. For d-Au collisions the most important geometrical scale comes from the r.m.s. radius of the deuteron and is correctly taken into account in the generation of the initial fireball.

In asymmetric systems, such as d-Au or p-Pb collisions, the fireball has no forward-backward reflection symmetry in rapidity around midrapidity. The multiplicity as function of pseudorapidity is higher on the side of the large nucleus. In the hydrodynamic model, the fireball lives longer and undergoes a stronger transverse expansion on that side [25]. The delay in the emission time of pions on the side of the larger nucleus gives observable effects for the interferometry correlations, a term combining the out and long directions appears in the Gaussian formula for the correlation function. The calculation predicts a nonzero value for the corresponding parameter  $R_{ol}^2$  in asymmetric d-Au or p-Pb collisions.

For central d-Au collisions the system is strongly asymmetric in azimuthal angle. The geometrical size is larger

out of plane and the transverse flow is stronger in plane. The effects of this asymmetry are clearly visible in azimuthally sensitive HBT analysis with respect to the second order event plane. The three HBT radii show a significant  $\cos(2\Phi)$  angular dependence. The second harmonic coefficient for the side radius is positive, as expected from the geometry of the emission source. The reverse is observed for the out direction,  $R_{o,2}^2$  is negative. The strong elliptic flow generates a small angular dependence in the long direction  $R_l$ . The out-side radius  $R_{os}^2$  is non-zero and proportional to  $\sin(2\Phi)$ .

The observed angular correlations in d-Au collisions [6] can originate from color glass condensate effects [26] or from the collective flow [3, 7, 27]. The experimental observation of the azimuthal dependence of the HBT radii with respect to the second order event plane would mean

that there is a correlation between the geometrical orientation of the fireball in d-Au collisions and the preferred flow direction. This would indicate that collective flow is the dominant source of the observed correlations, as the collective expansion translates the initial geometrical asymmetry into the azimuthal momentum asymmetry of the observed particles.

## ACKNOWLEDGMENTS

Supported by National Science Centre, Grant No. DEC-2012/05/B/ST2/02528 and by PL-Grid Infrastructure.

- 
- [1] A. M. Sickles, (2014), arXiv:1408.0220 [nucl-ex]; P. Bożek and W. Broniowski, Nucl.Phys. **A926**, 16 (2014), arXiv:1401.2367 [nucl-th]; R. Venugopalan, (2014), arXiv:1404.6976 [nucl-th].
  - [2] P. Bożek and W. Broniowski, Phys. Lett. **B720**, 250 (2013), arXiv:1301.3314 [nucl-th].
  - [3] A. Bzdak, B. Schenke, P. Tribedy, and R. Venugopalan, Phys. Rev. **C87**, 064906 (2013), arXiv:1304.3403 [nucl-th].
  - [4] B. B. Abelev *et al.* (ALICE Collaboration), (2014), arXiv:1404.1194 [nucl-ex]; S. Chatrchyan *et al.* (CMS), CMSPublic Web (2014), <http://twiki.cern.ch/twiki/bin/view/CMSPublic/PhysicsResultsHIN14013>.
  - [5] A. Adare *et al.* (PHENIX Collaboration), (2014), arXiv:1404.5291 [nucl-ex].
  - [6] A. Adare *et al.* (PHENIX Collaboration), Phys. Rev. Lett. **111**, 212301 (2013), arXiv:1303.1794 [nucl-ex].
  - [7] P. Bożek, Phys. Rev. **C85**, 014911 (2012), arXiv:1112.0915 [hep-ph].
  - [8] U. A. Wiedemann and U. W. Heinz, Phys. Rept. **319**, 145 (1999), arXiv:nucl-th/9901094; U. W. Heinz and B. V. Jacak, Ann. Rev. Nucl. Part. Sci. **49**, 529 (1999), arXiv:nucl-th/9902020; M. A. Lisa, S. Pratt, R. Soltz, and U. Wiedemann, Ann. Rev. Nucl. Part. Sci. **55**, 357 (2005), arXiv:nucl-ex/0505014.
  - [9] R. Nouicer *et al.* (PHOBOS), J. Phys. **G30**, S1133 (2004), arXiv:nucl-ex/0403033.
  - [10] G. Aad *et al.* (ATLAS), (2013), ATLAS-CONF-2013-096.
  - [11] S. Voloshin and W. Cleland, Phys.Rev. **C53**, 896 (1996), arXiv:nucl-th/9509025 [nucl-th]; U. A. Wiedemann, Phys.Rev. **C57**, 266 (1998), arXiv:nucl-th/9707046 [nucl-th]; M. A. Lisa, U. W. Heinz, and U. A. Wiedemann, Phys. Lett. **B489**, 287 (2000), arXiv:nucl-th/0003022; U. W. Heinz and P. F. Kolb, Phys.Lett. **B542**, 216 (2002), arXiv:hep-ph/0206278 [hep-ph].
  - [12] U. W. Heinz, A. Hummel, M. Lisa, and U. Wiedemann, Phys.Rev. **C66**, 044903 (2002), arXiv:nucl-th/0207003 [nucl-th].
  - [13] P. Bożek, Phys. Rev. **C85**, 034901 (2012), arXiv:1110.6742 [nucl-th].
  - [14] M. Rybczynski, G. Stefanek, W. Broniowski, and P. Bożek, Comput.Phys.Commun. **185**, 1759 (2014), arXiv:1310.5475 [nucl-th].
  - [15] P. Bożek, Phys. Rev. **C81**, 034909 (2010), arXiv:0911.2397 [nucl-th].
  - [16] S. Adler *et al.* (PHENIX Collaboration), Phys.Rev.Lett. **93**, 152302 (2004), arXiv:nucl-ex/0401003 [nucl-ex].
  - [17] J. Adams *et al.* (STAR Collaboration), Phys. Rev. **C71**, 044906 (2005), nucl-ex/0411036.
  - [18] Z. Chajecki, PhD thesis, Ohio State University, 2009.
  - [19] P. Bożek, Phys.Rev. **C89**, 044904 (2014), arXiv:1401.4894 [nucl-th].
  - [20] G. F. Bertsch, Nucl. Phys. **A498**, 173c (1989); S. Pratt, Phys. Rev. **D33**, 72 (1986).
  - [21] W. Broniowski, M. Chojnacki, W. Florkowski, and A. Kisiel, Phys. Rev. Lett. **101**, 022301 (2008), arXiv:0801.4361 [nucl-th]; S. Pratt, Phys. Rev. Lett. **102**, 232301 (2009), arXiv:arXiv: 0811.3363 [nucl-th] [nucl-th]; I. Karpenko, Y. Sinyukov, and K. Werner, Phys. Rev. **C87**, 024914 (2013), arXiv:1204.5351 [nucl-th].
  - [22] Y. Sinyukov, S. Akkelin, I. Karpenko, and V. Shapoval, Adv.High Energy Phys. **2013**, 198928 (2013); B. Tomasik, I. Melo, G. Torrieri, I. Mishustin, P. Bartos, *et al.*, Acta Phys.Polon.Supp. **1**, 513 (2008), arXiv:0712.0563 [nucl-th]; A. Bialas, W. Florkowski, and K. Zalewski, (2014), arXiv:1406.2499 [hep-ph].
  - [23] A. Białas and W. Czyż, Acta Phys. Polon. **B36**, 905 (2005), arXiv:hep-ph/0410265.
  - [24] J. Adams *et al.* (STAR Collaboration), Phys.Rev.Lett. **93**, 012301 (2004), arXiv:nucl-ex/0312009 [nucl-ex]; A. Adare *et al.* (PHENIX Collaboration), (2014), arXiv:1401.7680 [nucl-ex]; V. Loggins (ALICE Collaboration), (2014), arXiv:1408.0068 [nucl-ex].

- [25] P. Božek, A. Bzdak, and V. Skokov, Phys.Lett. **B728**, 662 (2014), arXiv:1309.7358 [hep-ph].
- [26] K. Dusling and R. Venugopalan, Phys. Rev. **D87**, 094034 (2013), arXiv:1302.7018 [hep-ph].
- [27] G.-Y. Qin and B. Müller, Phys.Rev. **C89**, 044902 (2014), arXiv:1306.3439 [nucl-th]; J. Nagle, A. Adare, S. Beckman, T. Koblesky, J. O. Koop, *et al.*, (2013), arXiv:1312.4565 [nucl-th].